Materials Science-Poland
http://www.materialsscience.pwr.wroc.pl/
DOI: 10.2478/msp-2021-0019

Klein–Nishina formula and Monte Carlo method for evaluating the gamma attenuation properties of Zn, Ba, Te and Bi elements

M.S. Al-Buriahi[1,*], Z.A. Alrowaili[2], Safa Ezzine[3], I.O. Olarinoye[4], Sultan Alomairy[5], C. Mutuwong[6], B. T. Tonguç[1]

[1]Department of Physics, Sakarya University, Sakarya, Turkey
[2]Department of Physics, College of Science, Jouf University, P.O.Box:2014, Sakaka, Saudi Arabia
[3]Department of Chemistry, College of Sciences, King Khalid University, P.O. Box 9004, Abha, Saudi Arabia
[4]Department of Physics, School of Physical Sciences, Federal University of Technology, Minna, Nigeria
[5]Department of Physics, College of Science, Taif University, P.O.Box 11099, Taif 21944, Saudi Arabia
[6]Department of Physics, Ubon Ratchathani University, Ubon Ratchathani, Thailand

In this work, the Klein–Nishina (K–N) approach was used to evaluate the electronic, atomic, and energy-transfer cross sections of four elements, namely, zinc (Zn), tellurium (Te), barium (Ba), and bismuth (Bi), for different photon energies (0.662 MeV, 0.835 MeV, 1.170 MeV, 1.330 MeV, and 1.600 MeV). The obtained results were compared with the Monte Carlo method (Geant4 simulation) in terms of mass attenuation and mass energy-transfer coefficients. The results show that the K–N approach and Geant4 simulations are in good agreement for the entire energy range considered. As the photon energy increased from 0.662 MeV to 1.600 MeV, the values of the energy-transfer cross sections decreased from 81.135 cm^2 to 69.184 cm^2 in the case of Bi, from 50.832 cm^2 to 43.344 cm^2 for Te, from 54.742 cm^2 to 46.678 cm^2 for Ba, and from 29.326 cm^2 to 25.006 cm^2 for Zn. The obtained results and the detailed information of the attenuation properties for the studied elements would be helpful in developing a new generation of shielding materials against gamma rays.

Keywords: *gamma ray, shielding, Monte Carlo, Klein–Nishina formula*

1. Introduction

Photons (X- and gamma- rays) are extensively used in medical intervention procedures for the sterilization of medical equipment, as well as therapeutic and diagnostic purposes, all over the world [1]. In fact, the health facilities and intervention procedures based on these radiations have increased in recent times. Many other industrial processes utilizing radiations have increased as well, such as medical applications [2], wastewater treatment [3], environmental protection [4], neutron irradiation [5], and applications of thin films [6]. Today, major diagnostic and therapeutic procedures involving the use of photons include diagnostic X-ray radiography, mammography, fluoroscopy, computed tomography (CT), brachytherapy, radiotherapy, and so on, all of which have increased environmental and personnel radiation doses considerably [7]. In view of the health hazards associated with exposing healthy tissues to radiation, the protection of patients, caregivers, and the general public is a fundamental aspect of a good quality assurance program (QAP), needed in all radiation facilities [8, 9]. At the heart of the QAP program are the following: the accurate detection of radiation and its measurement; and shielding systems. While the dosimetry system ensures prescribed dose compliance, a shield provides protection to healthy tissues, personnel, and the general public by confining radiation within a given space. Beyond the shield, doses are kept below the threshold of non-stochastic effects in living tissues.

Proper understanding of photon interaction

*E-mail: alburiahi@sakarya.edu.tr

mechanism and associated parameters is important if good choices of materials for accurate dose measurement and for the provision of an effective shield are to be made. The interaction parameters and mechanism illuminate our knowledge of how much photon penetrates or interacts with a medium and allows the quantification of energy deposited in the medium. Hence, photon interaction parameters are fundamental for determining the radiation dose and shielding competences of materials before their practical use.

Photon interactions leading to energy/photon absorption in the interacting medium come in three major forms, namely, photoelectric effect (PE), Compton scattering (CS), and pair production (PP). While the PE and PP lead to total absorption of photons, CS – on the other hand – offers more complex interaction procedures. Many radiation facilities produce and utilize photon beams whose energy ranges between a few keV and 5 MeV and where CS is a significant interaction process. Consequently, knowledge of the CS interaction processes and parameters of materials utilized for various functions (dosimetry, shielding, and so on) in these facilities is necessary. The CS of photons involves the inelastic collision of photons with atomic electrons. After the encounter, a photon transfers part of its energy to an electron and gets deflected from its initial path. If the energy transfer to the electron is greater than the electron's binding energy, the electron can be assumed to be free and at rest. The free electron approximation of the CS cross section is well described by the famous Klein–Nishina (K–N) formula [10]. The K–N theory is accurate for the evaluation of photon absorption and scattering cross sections of different materials for energies where CS dominates the interaction processes. These cross sections and energy-transfer coefficients are crucial for characterizing materials for dosimetry and shielding purposes [11]. Consequently, the present work describes the electronic, energy-transfer, and Compton cross sections for Zn, Ba, Te, and Bi using the K–N formula and Monte Carlo simulations. The evaluated parameters are useful for understanding and quantifying the photon absorption process of the chosen atoms with the view to assess their potential for shielding applications. The currently selected atoms (Zn, Ba, Te, and Bi) are the main ingredients of shielding materials that have shown superior abilities to many currently used shields [12–23].

In 2018, the electronic and CS cross sections of wax were evaluated for shielding purposes using the K–N equation. The study suggested that wax may not be ideal for shielding at high photon energies [24]. Moreover, Alexander et al. [25] adopted the K–N formula for the electronic cross section, CS attenuation, and energy-transfer coefficient of Pb, Cu, Co, Ca, and Al for radiation shielding and dosimetric applications. The study revealed that the cross sections and attenuation coefficients strongly depend on the photon energy and the ratio of the atomic number Z to the atomic weight A (Z/A ratio) of the interacting medium. It was concluded that controlling the Z/A ratio of a material can make it useful for radiation-shielding purposes. More recently, Thiele et al. [26] reported, using a modified K–N formula, the radiation shielding and dosimetry characteristics of Bi, W, Cd, Zn, Ni, and Fe. The report agreed with the study of Alexander et al. [25] that the electronic cross section depends on the Z of the interacting atoms, while CS attenuation strongly depends on the Z/A ratio of the atom. Clearly, these previous studies have shown that the K–N equation is a viable method for obtaining and analyzing photon interaction cross sections and attenuation coefficients.

Recently, there has been a growing continuous demand to develop new shielding materials for radiation applications in nuclear and medical facilities [26, 27]. The main ingredients of these materials are elements such as Zn, Te, Ba, and Bi, which have several superior physical and chemical properties in relation to other elements in the periodic table. For example, Al-Buriahi and Mann [28] studied the radiation shielding effect of some glass systems containing Te, Nb, and W. Alzahrani et al. [29] investigated the radiation protection features of a TeO_2–Na_2O–TiO glass system by using the Particle and Heavy ion Transport Code System (PHITS) Monte Carlo code. The findings of the studies show the importance of Te in the ability of the glass sample to shield the radiation. Al-Buriahi

et al. [30] also evaluated the nuclear protection ability of bismuth barium telluroborate glasses as dense and environment-friendly candidates. Their findings show the important role of Bi element in developing the glass system to shield from ionizing nuclear radiation. Therefore, this encouraged us to introduce a new method to study the radiation-shielding properties of the individual elements.

In the present article, the K–N approach has been used to evaluate the electronic, atomic, and energy-transfer cross sections of four elements, namely, zinc (Zn), tellurium (Te), barium (Ba), and bismuth (Bi), for different photon energies (0.662 MeV, 0.835 MeV, 1.170 MeV, 1.330 MeV, and 1.600 MeV). The results obtained by the K–N approach were compared with those determined by Geant4 Monte Carlo simulations.

2. Materials and methods

2.1. The K–N formula

The K–N formula is a very important approach to evaluate the differential cross section using the lowest order of quantum electrodynamics in the case of photon interactions with a single free electron. In the present work, we used the K–N approach for calculating the electronic, atomic, Compton, and energy-transfer cross sections as follows [24]:

$$ {}_e\sigma = 2\pi r_e^2 \left\{ \frac{1+\alpha}{\alpha^2} \left[\frac{2(1+\alpha)}{1+2\alpha} - \frac{\ln(1+2\alpha)}{\alpha} \right] + \right. $$
$$ \left. + \frac{\ln(1+2\alpha)}{2\alpha} - \frac{1+3\alpha}{(1+2\alpha)^2} \right\} \tag{1} $$

where ${}_e\sigma$ is the electronic cross section, $r_e = \frac{e^2}{4\pi\varepsilon_0 m_e c^2} = 2.818 \times 10^{-13}$ cm^2 is the radius of the electron, and $\alpha = \frac{E}{m_e c^2} = \frac{E}{0.511\text{MeV}}$ is a constant value called the "coupling strength" with E being the beam energy.

The K–N atomic cross section can be calculated by multiplying the results of Eq. (1) with the atomic number Z for the involved target [25]:

$$ {}_a\sigma = Z \cdot {}_e\sigma \tag{1a} $$

Then, the Compton mass attenuation coefficients can be estimated via the following expression:

$$ \sigma/\rho = \mathrm{N_A} \cdot \mathrm{Z} \cdot {}_e\sigma/\mathrm{A} \tag{1b} $$

The electronic mass energy-transfer cross sections can be calculated by solving the K–N equation, as shown below [25]:

$$ e^{tr} = 2\pi r_e^2 \left\{ \frac{2(1+\alpha)^2}{\alpha^2(1+2\alpha)} - \frac{1+3\alpha}{(1+2\alpha)^2} - \right. $$
$$ - \frac{(1+\alpha)\left(2\alpha^2-2\alpha-1\right)}{\alpha^2(1+2\alpha)^2} - \frac{4\alpha^2}{3(1+2\alpha)^3} - \tag{2} $$
$$ \left. - \left[\frac{1+\alpha}{\alpha^3} - \frac{1}{2\alpha} + \frac{1}{2\alpha^3} \right] \ln(1+2\alpha) \right\} $$

The atomic mass energy-transfer coefficient can be also calculated by multiplying the electronic mass energy-transfer cross sections with the charge number Z of each element:

$$ {}_a\sigma^{tr} = Z \cdot {}_e\sigma^{tr} \tag{2a} $$

The Compton mass energy-transfer coefficient is calculated using the methods in previous papers [24–26]:

$$ (\sigma/\rho)^{tr} = \mathrm{N_A} \cdot \mathrm{Z} \cdot {}_e\sigma^{tr}/\mathrm{A} \tag{2b} $$

2.2. Geant4 Monte Carlo simulation

In the present study, we used the Geant4 Monte Carlo approach to simulate and compare the results obtained using the K–N formula. Geant4 simulations can be carried out for several photon energies and different projectiles [27]. Such simulations have many advantages compared to the experimental work in terms of the accuracy of the outcomes and saving of time. Moreover, the validation of Geant4 simulation was achieved for several radiation studies and medical applications [28, 29].

All the simulation data and the theoretical data (obtained via the K–N formula) for important elements such as zinc (Zn), tellurium (Te), barium

(Ba), and bismuth (Bi) are new and cannot be found in the literature. With the current aim, we designed the required geometry to simulate the propagation of radiation through the elements involved. Figure 1 depicts the simulation geometry that was adopted, as described in the work of Al-Buriahi et al. [23, 27–29]. Using C++ language, we defined the elements involved and all the electromagnetic models that are needed to describe the photon interactions with the studied elements. Furthermore, in the input file of the Geant4 simulation, the detection area was defined to be NaI detector.

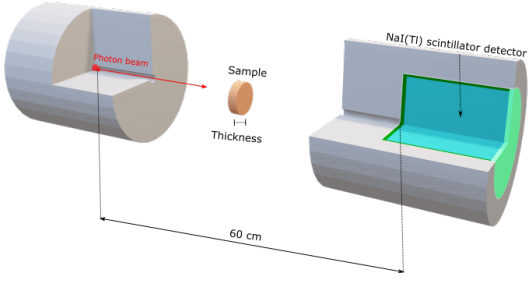

Fig. 1. The principal geometry for the present simulations by using Geant4.

3. Results and discussion

Table 1 shows the studied elements, namely, zinc (Zn), tellurium (Te), barium (Ba), and bismuth (Bi), along with their atomic numbers, atomic mass, and *Z*/*A* ratios. Such elements are very adaptable to the preparation and design of new materials for various applications related to radiation shielding. To use the K–N scattering equation for calculating the electronic cross sections of these elements, one has to evaluate the coupling strength (α) for each photon energy under study. The α values were calculated for six photon energies in the range of 0.662–1.600 MeV. The results of α are shown in Figure 2. Clearly, there is a direct linear relationship between the coupling strength and the photon energy. The maximum values of α were observed at 1.600 MeV with the value of 3.1311, while the minimum values of α were observed at 0.662 MeV, with the value of 1.2955.

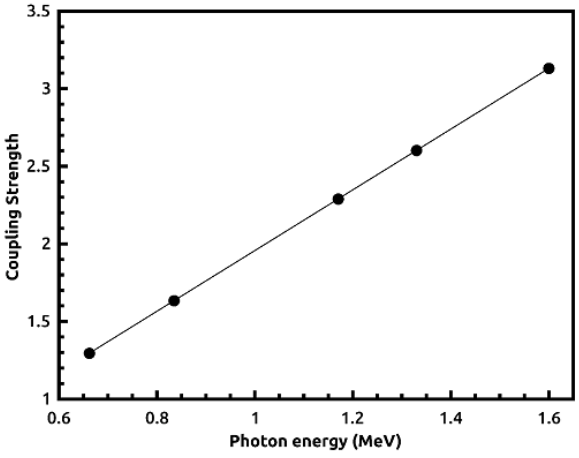

Fig. 2. Coupling strength as a function of photon energy.

Table 1. Studied elements along with their symbols, atomic numbers, atomic mass, and *Z*/*A* ratios.

Element	Symbol	*Z*	*A*	*Z*/*A*
Zinc	Zn	30	65.38	0.459
Tellurium	Te	52	127.60	0.408
Barium	Ba	56	137.33	0.408
Bismuth	Bi	83	208.98	0.397

Z/*A* ratio, the ratio of the atomic number *Z* to the atomic weight *A*.

The α values were then used to estimate the electronic, the atomic, and the Compton cross sections (otherwise called the Compton mass attenuation coefficient) for the studied elements according to Eqs. (1), (1a), and (1b). Table 2 shows the photon energy versus coupling constant, the K–N electronic cross section, and the electronic mass energy-transfer cross section. Figure 3 shows the variation of the K–N mass attenuation coefficients (σ/ρ) with the incident photon beam for the involved elements (Zn, Te, Ba, and Bi). It is noted that the σ/ρ values decrease with increasing beam energy. This decrease is due to the partial photon processes that have a strong relation with the energy. This behavior has been observed for several materials, such as glassy materials containing $TeO_2/Na_2O/TiO$ [29], environment-friendly telluroborate glasses [30], and $PbO/B_2O_3/Bi_2O_3/Fe_2O_3$ glasses [31]. In this

context, it is known that the PE (one of the partial photon processes) occurs at an energy of E<0.4 MeV, while CS dominates the partial photon processes in the energy range between 0.4 MeV and 5 MeV. Both PE ($\sim E^{-3}$) and CS ($\sim E^{-1}$) have an inverse proportion with energy. Therefore, the σ/ρ values were high at low energies and were low at high energies. This observation supports the results of the photon attenuation coefficient studies obtained by different methods and simulation codes [33–36].

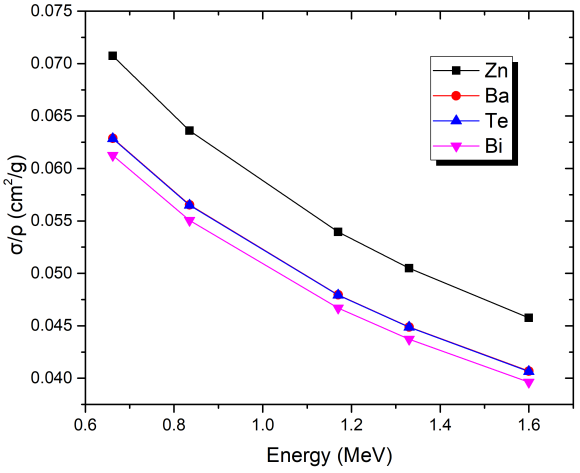

Fig. 3. K–N mass attenuation coefficients (σ/ρ) versus photon beam energy.

Table 2. Photon energy versus coupling constant (α), K–N electronic cross section ($_e\sigma$), and electronic mass energy-transfer ($_e\sigma^{tr}$) cross sections.

Source	Energy (MeV)	Coupling Strength (α)	$_e\sigma$ (cm^2/electron)	$_e\sigma^{tr}$ (cm^2/electron)
Cs-137	0.662	1.2955	2.56E–25	9.78E–26
Mn-54	0.835	1.6341	2.30E–25	9.55E–26
Co-60	1.170	2.2896	1.95E–25	9.02E–26
Co-60	1.330	2.6027	1.83E–25	8.76E–26
La-140	1.600	3.1311	1.66E–25	8.34E–26

K–N, Klein–Nishina.

Figure 4 demonstrates the behavior of the Compton mass attenuation coefficients with the Z/A ratio. Clearly, these coefficients increase linearly as the Z/A ratio increases. In Tables 3 and 4, the results from the use of the K–N scattering formula were compared with those extracted from the Geant4 simulations for all of the studied elements at photon energies of 0.662 MeV, 0.835 MeV, 1.170 MeV, 1.330 MeV, and 1.600 MeV. This comparison is presented in terms of the Compton scattering mass coefficients for Zn and Ba elements in Table 3 and for Te and Bi elements in Table 4. Generally, there is good agreement between the results of the K–N scattering formula and the Geant4 simulations. For example, the highest percentage deviation (Dev.%) was < 2% for the photon energy of 0.662 MeV in the case of Bi (see Table 4). From Table 3, in the case of Zn, the Dev.% values were 0.851, 0.944, 0.824, 0.697, and 0.504 for photon energies of 0.662 MeV, 0.835 MeV, 1.170 MeV, 1.330 MeV, and 1.600 MeV, respectively. The maximum Dev.% values were 0.944 at 0.835 MeV for Zn, 1.234 at 0.662 MeV for Ba, 1.204 at 0.835 MeV for Te, and 1.714 at 0.835 MeV for Bi.

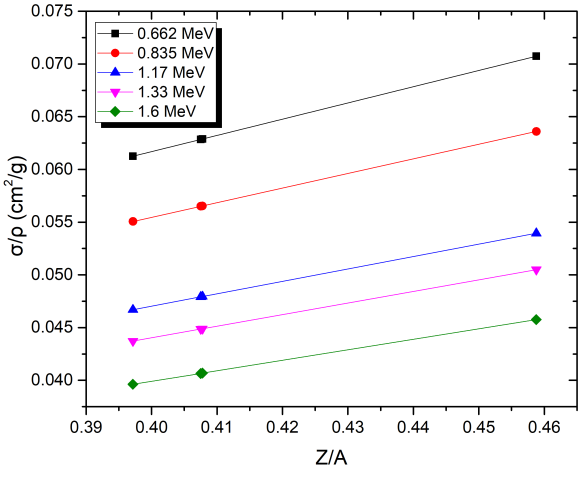

Fig. 4. Variation in the Compton mass attenuation coefficients (σ/ρ) as a function of the atomic number Z and the atomic weight A, i.e., the Z/A ratio.

Figure 5 shows the relation between the K–N energy-transfer cross section and the photon energy. It is seen that, for a given element, the energy-transfer cross section decreases with increase in the photon energy. As the photon energy increased from 0.662 MeV to 1.600 MeV, the values of

Table 3. Compton mass attenuation coefficients for Zn and Ba obtained by using Geant4 simulations and K–N scattering formula.

Energy (MeV)	Zn			Ba		
	K–N	Geant4	Dev.%	K–N	Geant4	Dev.%
6.62E–01	0.071	0.071	0.851	0.062	0.063	1.234
8.35E–01	0.063	0.064	0.944	0.056	0.057	1.231
1.17E+00	0.054	0.054	0.824	0.048	0.048	1.138
1.33E+00	0.051	0.051	0.697	0.045	0.045	0.946
1.60E+00	0.046	0.046	0.504	0.041	0.041	0.782

Dev.%, percentage deviation; K–N, Klein–Nishina.

Table 4. Compton mass attenuation coefficients for Te and Bi elements obtained by using Geant4 simulations and K–N scattering formula.

Energy (MeV)	Te			Bi		
	K–N	Geant4	Dev.%	K–N	Geant4	Dev.%
6.62E–01	0.062	0.063	1.079	0.060	0.061	1.706
8.35E–01	0.056	0.057	1.204	0.055	0.055	1.714
1.17E+00	0.048	0.048	0.997	0.046	0.047	1.501
1.33E+00	0.045	0.045	0.951	0.044	0.044	1.339
1.60E+00	0.041	0.041	0.721	0.040	0.040	1.070

Dev.%, percentage deviation; K–N, Klein–Nishina.

the energy-transfer cross sections decreased from 81.135 cm^2 to 69.184 cm^2 in the case of Bi, from 50.832 cm^2 to 43.344 cm^2 for Te, from 54.742 cm^2 to 46.678 cm^2 for Ba, and from 29.326 cm^2 to 25.006 cm^2 for Zn.

Figure 6 represents the relation between the K–N mass energy-transfer coefficients and the photon energy. This figure provides detailed information about the energy-transfer cross section of the studied elements at different photon energies. Clearly, there is a linear relation with a small slope between the energy-transfer cross section and the photon energy for all of the studied elements. Such behavior can be attributed to the trend of the *Z*/*A* ratio, which has to be $0.39 < Z/A < 0.5$ for stable elements [25]. Furthermore, there is a remarkable decrease in this cross section with increase in the photon energy from 0.662 MeV to 1.6 MeV. This indicates that the highest attenuation of the photon beams occurs at the low-energy region.

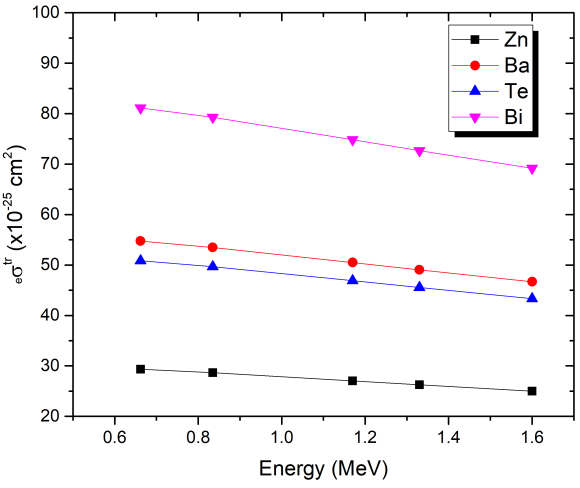

Fig. 5. K–N electron-transfer cross section ($_e\sigma^{tr}$) as a function of the energy of interacting γ-rays. K–N, Klein–Nishina.

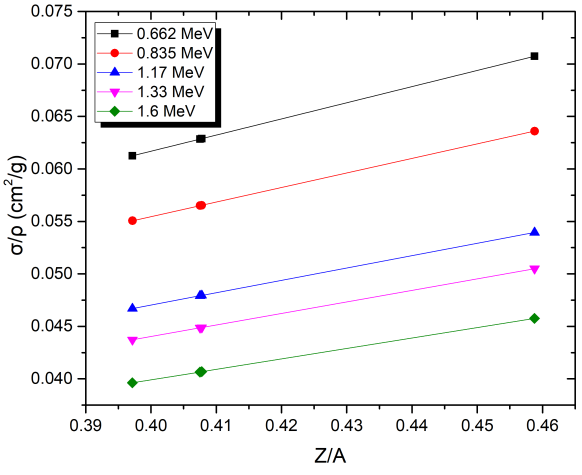

Fig. 6. Change in the K–N mass energy-transfer coefficients as a function of the *Z*/*A* ratio of the elements. K–N, Klein–Nishina; *Z*/*A* ratio, the ratio of the atomic number *Z* to the atomic weight *A*.

Moreover, there is a weak dependence on the *Z*/*A* ratio for a given element. For example, as the photon energy varies from 0.662 MeV to 1.600 MeV, the energy-transfer coefficients varied from 0.0270 cm^2/g to 0.0230 cm^2/g for Zn, from 0.0240 cm^2/g to 0.0205 cm^2/g for Ba, from 0.0240 cm^2/g to 0.0204 cm^2/g for Te, and from 0.0234 cm^2/g to 0.0199 cm^2/g for Bi.

4. Conclusion

In the present study, we have reported the electronic, energy-transfer, and Compton cross sections for Zn, Te, Ba, and Bi obtained by using K–N scattering formula and Geant4 simulations at photon energies of 0.662 MeV, 0.835 MeV, 1.170 MeV, 1.330 MeV, and 1.600 MeV. The highest deviation between the results of the K–N approach and Geant4 simulations was <2% for the photon energy of 0.662 MeV in the case of Bi. The maximum value of α (3.1311) was observed at 1.600 MeV, while the minimum value of α (1.2955) was observed at 0.662 MeV. The energy-transfer coefficients varied from 0.0270 cm^2/g to 0.0230 cm^2/g for Zn, from 0.0240 cm^2/g to 0.0205 cm^2/g for Ba, from 0.0240 cm^2/g to 0.0204 cm^2/g for Te, and from 0.0234 cm^2/g to 0.0199 cm^2/g for Bi. Knowing and controlling the shielding properties of the studied elements would be very helpful in preparing and developing new advanced materials for gamma-ray-shielding applications.

Acknowledgements

We would like to thank Taif University Research Supporting Project number (TURSP-2020/63), Taif University, Taif, Saudi Arabia. Moreover, the authors express their appreciation to the Deanship of Scientific Research (DSR), King Khalid University, Abha, Saudi Arabia for funding this work through the General Research Project, under grant No. G.R.P-167-41.

References

[1] Ogundare FO, Olarinoye IO, Obed RI. Estimation of patients' organ doses and conceptus doses from selected X-ray examinations in two Nigeria X-ray centers. Radiat Prot Dosimetry. 2008;132(4):395–2.

[2] Institute of Medicine (US) Committee for Review and Evaluation of the Medical Use Program of the Nuclear Regulatory Commission; Gottfried KLD, Penn G, editors. Radiation in medicine: A need for regulatory reform. Washington (DC): National Academies Press (US); 1996. 2, Clinical Applications of Ionizing Radiation. Available from: https://www.ncbi.nlm.nih.gov/books/NBK232715/

[3] Rahman ROA, Hung YT. Application of ionizing radiation in wastewater treatment: An overview. Water. 2020; 12(1):19.

[4] Chmielewski A. Application of ionizing radiation to environment protection. Nukleonika. 2005;50:17–4.

[5] Olarinoye IO, Ogundare FO. Optical and microstructural properties of neutron irradiated RF-sputtered amorphous alumina thin films. Optik. 2017;134:66–77.

[6] Ogundare FO, Olarinoye IO. He^+ induced changes in the surface structure and optical properties of RF-sputtered amorphous alumina thin films. J Non Crystalline Solids. 2016;432:292–9.

[7] Sulieman A, Adam H, Elnour A, Tamam N, Alhaili A, Alkhorayef M, et al. Patient radiation dose reduction using a commercial iterative reconstruction technique package. Radiat Phys Chem. 2021;178:108996.

[8] Valentin J. Avoidance of radiation injuries from medical interventional procedures, ICRP Publication 85. Ann ICRP. 2000;30(2):7–67.

[9] Cousins C, Miller DL, Bernardi G, Rehani MM, Schofield P, Vañó E, et al. ICRP PUBLICATION 120: Radiological protection in cardiology. Ann ICRP. 2013;42(1):1–125.

[10] Attix FH. Introduction to radiological physics and radiation dosimetry. John Wiley & Sons; 2008.

[11] Thiele KT, Alexander RW, Maqbool M. Characterization of 83Bi209, 74W184, 48Cd112, 30Zn65, 28Ni59 and 26Fe56 using Modified Klein-Nishina formula, for radiation shielding and dosimetry. Radiat Phys Chem. 2021;179:109264.

[12] Al-Buriahi MS, El-Agawany FI, Sriwunkum C, Akyıldırım H, Arslan H, Tonguc BT,et al. Influence of Bi_2O_3/PbO on nuclear shielding characteristics of lead-zinc-tellurite glasses. Phys B 2020;581:411946.

[13] Al-Buriahi MS, Gaikwad DK, Hegazy HH, Sriwunkum C, Algarni H. Newly developed glasses containing Si/Cd/Li/Gd and their high performance for radiation applications: Role of Er_2O_3. J Mater Sci. 2021;32(7):9440–51.

[14] Alalawi A, Al-Buriahi MS, Sayyed MI, Akyildirim H, Arslan H, Zaid MH, et al. Influence of lead and zinc oxides on the radiation shielding properties of tellurite glass systems. Ceram Int. 2020;46(11):17300–6.

[15] TekinHO, Issa SA, Mahmoud KAA, El-Agawany FI, Rammah YS, Susoy G, et al. Nuclear radiation shielding competences of barium-reinforced borosilicate glasses. Emerg Mater Res. 2020;9(4):1131–44.

[16] Boukhris I, Kebaili I, Al-Buriahi MS, Alalawi A, Abouhaswa AS, Tonguc B. Photon and electron attenuation parameters of phosphate and borate bioactive glasses by using Geant4 simulations. Ceram Int. 2020;46(15):24435–42.

[17] Kebaili I, Boukhris I, Al-Buriahi MS, Alalawi A, Sayyed MI. Ge-Se-Sb-Ag chalcogenide glasses for nuclear radiation shielding applications. Ceram Int. 2021;47(1):1303–9.

[18] Boukhris I, Kebaili I, Al-Buriahi MS, Sriwunkum C, Sayyed MI. Effect of lead oxide on the optical properties and radiation shielding efficiency of antimony-sodium-tungsten glasses. Appl Phys A. 2020;126(10):1–0.

[19] Agostinelli S, Allison J, Amako KA, Apostolakis J, Araujo H, Arce P, et al. GEANT4–a simulation toolkit. Nucl Instrum. 2003;506(3):250–3.

[20] Lakshminarayana G, Dong MG, Al-Buriahi MS, Kumar A, Lee DE, Yoon J, et al. B_2O_3–Bi_2O_3–TeO_2–BaO and

TeO_2–Bi_2O_3–BaO glass systems: A comparative assessment of gamma-ray and fast and thermal neutron attenuation aspects. Appl Phys A. 2020;126(3):1–18.

[21] Creagh DC, Hubbell JH. Problems associated with the measurement of X-ray attenuation coefficients. I. Silicon. Report of the International Union of Crystallography X-ray Attenuation Project. Acta Cryst. 1987;43(1):102–12.

[22] Al-Buriahi M S, Arslan H, Tonguç BT. Mass attenuation coefficients, water and tissue equivalence properties of some tissues by Geant4, XCOM and experimental data. Indian J Pure Appl Phys. 2019;57(6):433–7.

[23] Al-Hadeethi Y, Al-Buriahi MS, Sayyed MI. Bioactive glasses and the impact of Si_3N_4 doping on the photon attenuation up to radiotherapy energies. Ceram Int. 2020;46(4):5306–14.

[24] Alenezi M, Stinson K, Maqbool M, Bolus N. Klein–Nishina electronic cross-section, Compton cross sections, and buildup factor of wax for radiation shielding and protection. J Radiol Prot. 2018;38(1):372.

[25] Alexander RW, Thiele KT, Maqbool M. Electronic cross-sections and Compton attenuation and transfer coefficients of 82Pb208, 29Cu64, 27Co59, 20Ca40 and 13Al27 for applications in radiation shielding and dose. Phys Scripta. 2020;95(8):085006.

[26] Thiele KT, Alexander RW, Maqbool M. Characterization of 83Bi209, 74W184, 48Cd112, 30Zn65, 28Ni59 and 26Fe56 using Modified Klein-Nishina formula, for radiation shielding and dosimetry. Radiat Phys Chem. 2021;179:109264.

[27] Al-Buriahi MS, Singh VP. Comparison of shielding properties of various marble concretes using GEANT4 simulation and experimental data. J Aust Ceram Soc. 2020;56(3):1127–33.

[28] Al-Buriahi MS, Mann KS. Radiation shielding investigations for selected tellurite-based glasses belonging to the TNW system. Mater Res Express. 2019;6(10):105206.

[29] Alzahrani JS, Alothman MA, Eke C, Al-Ghamdi H, Aloraini DA, Al-Buriahi MS. Simulating the radiation shielding properties of TeO_2–Na_2O–TiO glass system using PHITS Monte Carlo code. Comput Mater Sci. 2021;196:110566.

[30] Al-Buriahi MS, Olarinoye IO, Alomairy S, Kebaili I, Kaya R, Arslan H, et al. Dense and environment friendly bismuth barium telluroborate glasses for nuclear protection applications. Prog Nucl Energy. 2021;137:103763.

[31] Sekhar KC, Hameed A, Narsimlu N, Alzahrani JS, Alothman MA, Olarinoye IO, et al. Synthesis, optical, structural, and radiation transmission properties of $PbO/Bi_2O_3/B_2O_3/Fe_2O_3$ glasses: An experimental and in silico study. Optical Mater. 2021;117:111173.

[32] Olarinoye IO, Alomairy S, Sriwunkum C, Hegazy HH, Al-Buriahi MS. Effects of TeO_2 and B_2O_3 on photon, neutron, and charged particle transmission properties of Bi_2O_3-BaO-LiF glass system. J Aust Ceram Soc. 2021:1–2.

[33] Al-Buriahi MS, Alzahrani JS, Olarinoye IO, Mutuwong C, Elsaeedy HI, Alomairy S, et al. Effects of reducing PbO content on the elastic and radiation attenuation properties of germanate glasses: A new non-toxic candidate for shielding applications. J Mater Sci. 2021;32(11):15080–94.

[34] Al-Buriahi MS, Alomairy S, Mutuwong C. Effects of MgO addition on the radiation attenuation properties of 45S5 bioglass system at the energies of medical interest: An in silico study. J Aust Ceram Soc. 2021:1–9.

[35] Al-Buriahi M S, Tonguc BT. Mass attenuation coefficients, effective atomic numbers and electron densities of some contrast agents for computed tomography. Radiat Phys Chem. 2019:108507.

[36] Al-Buriahi MS, Eke C, Alomairy S, Mutuwong C, Sfina N. Micro-hardness and gamma-ray attenuation properties of lead iron phosphate glasses. J Mater Sci. 2021:1–1.

Received 19-04-2021
Accepted 20-08-2021